Published in Optical Engineering 34, issue 12, 3456-3464, 1995
which should be used for any reference to this work

Continuous-relief fan-out elements with optimized fabrication tolerances

Peter Ehbets,* MEMBER SPIE
University of Neuchâtel
Institute of Microtechnology
Rue A.-L. Breguet 2
CH-2000 Neuchâtel, Switzerland
E-mail: ehbets@imt.unine.ch

Markus Rossi
Paul Scherrer Institute Zurich
Badenerstrasse 569
CH-8048 Zurich, Switzerland

Hans Peter Herzig
University of Neuchâtel
Institute of Microtechnology
Rue A.-L. Breguet 2
CH-2000 Neuchâtel, Switzerland

Abstract. The design of kinoform fan-out elements with high efficiency and reduced sensitivity to vertical profile scaling errors is presented. We start from a high-efficiency continuous-phase fan-out solution and optimize the position of the 0-2π transitions in the phase function, in order to achieve a high fabrication-error tolerance. The sensitivity of Fourier-transform and focusing fan-out elements to vertical etch-depth errors is analyzed. The limitations for the fabrication of such structures by laser-beam writing are discussed. In particular, the influence of the finite writing-spot diameter on the fan-out performance is investigated. Design rules for fan-out elements, which consider fabrication constraints, are derived. Experimental results are presented for cylindrical focusing fan-out elements with small uniformity error (2%) and weak profile scaling dependence.

Subject terms: kinoform; fan-out; diffractive optics; laser-beam writing.

1 Introduction

Space-invariant fan-out elements are key components for optical interconnections and also find applications in optical sensors and in material processing. They split an incoming laser beam into an array of diffraction orders of equal power, which are focused by a Fourier-transform lens. The requirements on fan-out elements are high efficiency and, in general, a uniformity error in the generated spot array below 10%.

On-axis diffractive optical elements (DOEs) with high diffraction efficiency require the fabrication of a kinoform, which can be realized by either a continuous[1] or a multilevel[2] surface-relief grating structure. Unfortunately, low uniformity errors require very accurate fabrication of the surface-relief profile, which is difficult to achieve with both techniques.[1,3] As a consequence, fabrication-error tolerances are important and have to be included in the design process of kinoform elements.

In this paper, we concentrate on the design of continuous-relief fan-out elements that can be fabricated by laser beam writing. Alternative fabrication approaches for such structures are direct electron-beam writing[4] and gray-tone mask lithography.[5] These technologies produce the desired surface relief in a single lithographic step. Therefore, they can achieve high lateral positioning accuracy. However, vertical profile depth errors are more difficult to control and are mainly responsible for poor fan-out performance. The goal of this paper is to present a design approach for continuous-relief fan-out elements that have high diffraction efficiency and reduced sensitivity of the fan-out reconstruction quality to vertical profile depth errors.

In Sec. 2 we review the design of highly efficient fan-out gratings. In addition, we consider the inclusion of focusing power in the fan-out element. The combination of multiple beamsplitting and focusing in a single planar DOE enables the realization of compact micro-optical systems. In Sec. 3 we analyze the sensitivity of Fourier-transform and focusing fan-out elements to profile depth scaling errors. In Sec. 4 fabrication by laser-beam writing is discussed, and the influence of the finite writing-spot diameter on the fan-out performance is analyzed. Finally, in Sec. 5, experimental results for cylindrical focusing fan-out elements with small profile scaling dependence are presented.

2 Design of Fan-out Elements

We restrict the discussion for the following to a one-dimensional geometry. The extension to the two-dimensional case is straightforward. The goal of the fan-out design process is to determine a phase function $\phi_f(x)$ that equalizes and maximizes the power in the N fan-out diffraction orders, which are defined by the Fourier coefficients

$$A_p = \frac{1}{d}\int_0^d \exp[i\phi_f(x)] \exp\left(-\frac{i2\pi px}{d}\right) dx \ , \qquad (1)$$

where d is the grating period. In order to achieve the highest diffraction efficiency, we use the phases of the complex amplitudes of the diffraction orders A_p as free optimization pa-

*Current affiliation: Institut National d'Optique (INO), #69, Rue Franquet Sainte-Foy, Quebec, G1P 4N8, Canada.

rameters and calculate, as described in Refs. 1, 6, and 7, an analog phase function $\phi_f(x)$. For the optimization process, we describe the quality of an $N\times 1$ fan-out function $\phi_f(x)$ by the diffraction efficiency

$$\eta = \sum_{p=1}^{N} I_p \Big/ \sum_{p=-\infty}^{\infty} I_p \tag{2}$$

and by the uniformity error

$$\sigma = \frac{I_{\max} - I_{\min}}{I_{\max} + I_{\min}} , \tag{3}$$

where $I_{\max}$, $I_{\min}$, represent the maximum and minimum intensities of the N fan-out diffraction orders $I_p = |A_p|^2$. For regular fan-out elements (no suppressed diffraction orders in the fan-out pattern), high diffraction efficiencies over 90% are achieved. The dashed curve in Fig. 1 shows one period of the continuous phase function $\phi_f(x)$ for a 9×1 fan-out element, which produces the fan-out pattern with a diffraction efficiency of $\eta = 99.3\%$ and perfect uniformity.

2.1 *Focusing Fan-out Elements*

A focusing fan-out element performs simultaneously the multiple beamsplitting and the focusing operation. We assume illumination with a monochromatic plane wave and consider the readout geometry for a transmissive focusing fan-out element shown in Fig. 2. In this case, the phase function of the focusing fan-out element is the combination of the periodic Fourier-transform fan-out function $\phi_f(x)$ and a spherical phase function $\phi_s(x)$. Using paraxial scalar diffraction theory,[8] the focusing fan-out element is described by the complex-amplitude transmittance function

$$t(x;\lambda_0) = P(x)\ \exp\{i[\phi_f(x) + \phi_s(x)]\} , \tag{4}$$

where λ_0 is the design wavelength in free space, $P(x) = \mathrm{rect}(x/D)$ is the rectangular aperture of diameter D, and the spherical phase function $\phi_s(x)$ can be written in the paraxial approximation as

$$\phi_s(x) = -\frac{\pi x^2}{\lambda_0 f} , \tag{5}$$

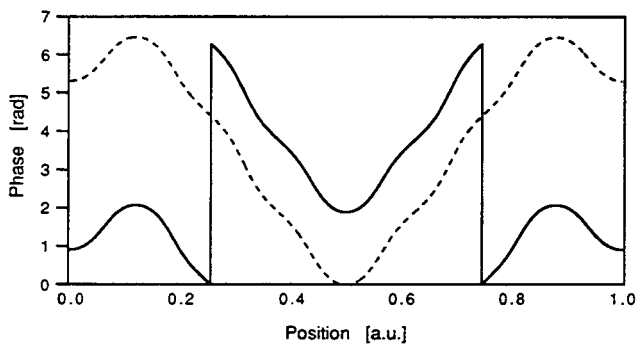

Fig. 1 One period of the efficiency-optimized phase function for the 9×1 fan-out element. Dashed curve: continuous phase function; solid curve: phase function with 0–2π transitions, optimized for highest profile scaling-error tolerance.

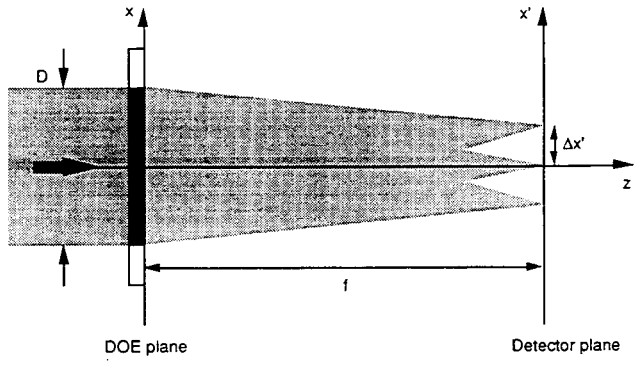

Fig. 2 Readout geometry for a transmissive focusing fan-out element.

where f is the focal length. The field propagation to the detection plane is then described by the Fresnel diffraction integral

$$U(x',z) = \frac{\exp(ikz)}{\sqrt{i\lambda z}} \int_{-\infty}^{\infty} t(x;\lambda)\ \exp\left[i\frac{k}{2z}(x'-x)^2 \right] dx , \tag{6}$$

where $k = 2\pi/\lambda$ and λ is the readout wavelength. Inserting Eqs. (4) and (5) into Eq. (6) and using $\lambda = \lambda_0$, the field distribution $U(x', z=f)$ in the focal plane at $z=f$ becomes essentially the Fourier transform (FT) of the fan-out phase function $\phi_f(x)$:

$$U(x', z=f) \propto \mathrm{FT}\left\{ \mathrm{rect}\left(\frac{x}{D}\right)\ \exp[i\phi_f(x)] \right\}$$

$$= \sum_{p=-\infty}^{\infty} A_p\ \mathrm{sinc}\left[\frac{D}{\lambda_0 f}\left(x' - \frac{p\lambda_0 f}{d} \right) \right] , \tag{7}$$

where $\mathrm{sinc}x = (\sin\pi x)/(\pi x)$. The spot spacing $\Delta x'$ in the focal plane becomes

$$\Delta x' = \frac{\lambda_0 f}{d} . \tag{8}$$

In order to separate the spots and not to introduce noise, several periods of the fan-out element have to be illuminated. In particular, we chose the aperture diameter D to be an integer multiple of the fan-out period d, i.e., $D = Md$ with $M > 10$. The efficiency η and the uniformity error u of the focused-spot array are then determined by the quality of the initial fan-out function $\phi_f(x)$. Figure 3 shows the calculated irradiance distribution $I(x', z=f) = |U(x', z=f)|^2$ for a 9×1 focusing fan-out element with $D = 2.56$ mm, $\lambda_0 = 632.8$ nm, $d = 160$ μm, and $f = 25$ mm, which results in a spot spacing in the focal plane of $\Delta x' = 99$ μm. The 9×1 focusing fan-out element yields a maximum diffraction efficiency of $\eta = 99.3\%$ and perfect uniformity.

The realization of the transmittance function $t(x;\lambda_0)$ as a planar surface-relief DOE requires the wrapping of the phase function in Eq. (4) to an interval between 0 and an integer multiple of 2π. In the following, without loss of generality, we restrict the discussion to the case of a maximum modu-

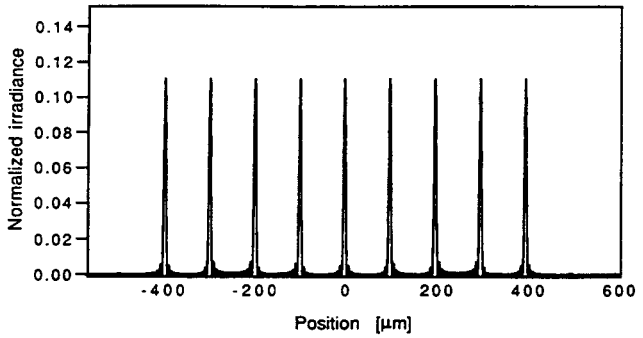

Fig. 3 Calculated irradiance distribution in the focal plane of the focusing 9×1 fan-out element.

lation depth equal to 2π. Therefore, the maximum depth h of the corresponding surface-relief grating structure becomes

$$h=\frac{\lambda_0}{n(\lambda_0)-1} , \tag{9}$$

where n is the refractive index of the grating material. The resulting phase function $\Psi(x)$ of the element can then be written as

$$\Psi(x)=[\phi_f(x)+\phi_s(x)+\varphi_0] \bmod 2\pi , \tag{10}$$

where φ_0 is a constant phase offset. The consequences of the phase wrapping are discrete transitions from 0 to 2π in the phase profile. Using the phase offset φ_0 in Eq. (10), the position of the transition points can be shifted laterally. This has no effect on the fan-out quality for an ideal element with the calculated phase function $\Psi(x)$ of Eq. (10). However, as we show in the next section, the fabrication error tolerances for the kinoform surface-relief element, which generates the phase function $\Psi(x)$, depend strongly on the position of the transition points. Therefore, the phase offset φ_0 can be used efficiently to reduce the sensitivity of the kinoform element to fabrication errors.

3 Fabrication Error Tolerances

In this section, we consider the influence of vertical etch-depth errors on the reconstruction quality of the ideal fan-out phase function $\Psi(x)$ and minimize the sensitivity of the fan-out function to such fabrication errors.

For the analysis, we assume a linear scaling of the phase function $\Psi(x)$, which can result from either a wavelength change ($\lambda \neq \lambda_0$) or a linear surface relief error. The scaling results in the new transmittance function

$$t_s(x;\lambda)=P(x)\ \exp[i\alpha\Psi(x)] , \tag{11}$$

where α represents the linear scaling factor, which for a surface-relief DOE in transmission has the form

$$\alpha=\frac{\lambda_0[n(\lambda)-1]}{\lambda[n(\lambda_0)-1]}\beta . \tag{12}$$

The first factor in Eq. (12) takes into account the wavelength and material dispersion dependence,[9] and β represents the relief depth scaling. In order to understand the influence of the scaling errors on the fan-out performance, it is useful to note that the scaled phase function $\alpha\Psi(x)$ has the same periodicity as the ideally wrapped phase function $\Psi(x)$. As a consequence, the transmittance function of the scaled element $t_s(x;\lambda)$ can be expressed[10,11] by a generalized Fourier series expansion of the variable $\Psi(x)$:

$$t_s(x;\lambda)=P(x)\sum_{q=-\infty}^{\infty} B_q\ \exp[iq\Psi(x)] , \tag{13}$$

where the coefficients are given by

$$B_q=\frac{1}{2\pi}\int_0^{2\pi} \exp[i(\alpha-q)\Psi(x)]\ d\Psi(x)$$

$$=\exp[i\pi(\alpha-q)]\ \operatorname{sinc}(\alpha-q) . \tag{14}$$

The $q=1$ term in Eq. (13) corresponds to the desired fan-out signal. As a consequence, scaling errors do not influence the optimized phase function $\Psi(x)$, but they reduce the power in the signal wave by a factor $|B_1|^2=\operatorname{sinc}^2(\alpha-1)$ and produce additional noise orders ($q\neq 1$) with amplitudes B_q, which affect the fan-out signal through interference. Inserting Eqs. (10) and (14) into Eq. (13), we can rewrite the transmittance function of the scaled element as

$$t_s(x;\lambda)=P(x)\sum_{q=-\infty}^{\infty} \exp[iq(\varphi_0-\pi)]\ \operatorname{sinc}(\alpha-q)$$

$$\times\exp\{iq[\phi_f(x)+\phi_s(x)]\} , \tag{15}$$

where multiplicative phase factors have been omitted. The constant phase offset φ_0 changes the relative phase of the different orders q in Eq. (15) and can be used to minimize the interference effects without reducing the high diffraction efficiency η of the initial fan-out function $\phi_f(x)$.

In order to define a criterion for the sensitivity of the fan-out function to scaling errors, we calculate the average diffraction efficiency

$$\eta_s=0.5[\eta(\alpha=0.9)+\eta(\alpha=1.1)] \tag{16}$$

and the average uniformity error

$$\sigma_s=0.5[u(\alpha=0.9)+u(\alpha=1.1)] , \tag{17}$$

resulting from scaling factors $\alpha=0.9$ and $\alpha=1.1$.

This criterion corresponds to a large tolerable scaling error of $\pm 10\%$, which can be achieved even in an industrial fabrication environment. It follows from Eq. (15) that the power in the signal fan-out order is reduced by the factor $|B_1|^2=\sin^2(0.1)=0.9675$, and the spurious noise orders contain 3.25% of the total power. In the next two subsections, we have investigated numerically the sensitivity of the efficiency η_s and of the uniformity error u_s to scaling errors for Fourier-transform and focusing fan-out elements.

3.1 *Fourier-Transform Fan-Out Elements*

We first have analyzed the scaling-error sensitivity of Fourier-transform fan-out elements [$\phi_s(x)=0$]. Using direct write technologies, the continuous phase function $\phi_f(x)$ of a

Fourier-transform fan-out element can either be directly realized or be wrapped to the interval $[0, 2\pi]$ for the fabrication. Both possibilities are shown in Fig. 1. In the ideal case, both approaches yield the same efficiency and uniformity. However, as will be shown in the following analysis, they have a fundamentally different response to scaling errors.

In the case of continuous-phase DOEs without discrete phase transitions, scaling errors modify directly the fan-out phase function $\phi_f(x)$ and therefore affect directly the angular spectrum of the diffraction orders in Eq. (1). The generalized Fourier expansion in Eq. (15) is not valid for continuous phase functions. As a consequence, a strong dependence of the uniformity error on scaling errors results. We have calculated the far field of the scaled continuous fan-out phase function $\exp\{i\alpha\phi_f(x)\}$. The sensitivity criterion [Eq. (17)] produces a uniformity error of $\sigma_s = 46\%$ for the 9×1 fan-out element and of $\sigma_s = 91\%$ for a 45×1 fan-out element. In the absence of scaling errors ($\alpha = 1.0$), both optimized fan-out elements generate a uniformity error σ below 0.1%.

In order to analyze Fourier-transform fan-out elements with the wrapped phase function, the Fraunhofer diffraction pattern of the scaled transmittance function $t_s(x;\lambda)$ in Eq. (15) has to be calculated. Since the fan-out phase function is periodic, the Fraunhofer diffraction pattern is a discrete function. Therefore, the fan-out diffraction orders and spurious noise orders are overlapping, and interference effects are expected. The dashed curve in Fig. 4 shows the sensitivity σ_s of the uniformity error for the 9×1 fan-out element as a function of the phase offset φ_0. For comparison, we have also plotted the uniformity-error sensitivity σ_s of the continuous phase function without discrete transitions. It is shown that by choosing an optimum value for φ_0, the interference effects between the fan-out orders and the spurious noise orders are minimized and the uniformity-error sensitivity σ_s is reduced from over 40% to 8%. The phase function of the 9×1 fan-out element with the location of the transition points optimized to get minimum scaling error is represented in Fig. 1 by the solid line. Similar results have been obtained for fan-out elements with fan-out numbers $N \leq 9$. For larger fan-out numbers N, the uniformity error sensitivity u_s can be reduced by a similar amount, but no longer below 10%. This result can be seen in Fig. 5 for the 45×1 fan-out element, where only a minimum uniformity sensitivity of $\sigma_s = 30\%$ is achieved.

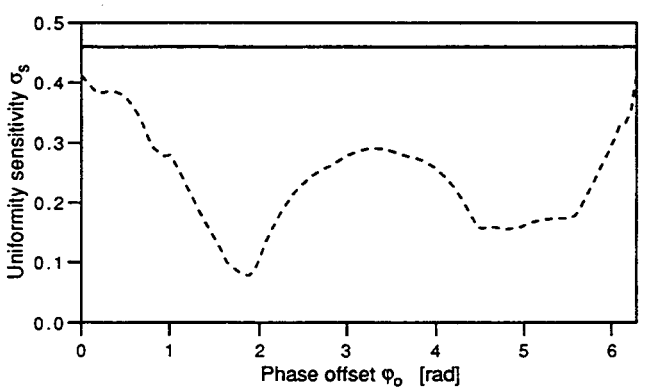

Fig. 4 Uniformity error sensitivity σ_s for the 9×1 fan-out element as a function of the phase offset parameter φ_0 for a phase function with 0–2π transitions (dashed curve). The value of σ_s for the continuous phase function is indicated for comparison (solid curve).

The main problem for the remaining large uniformity error is the interference with the zero-order term of the generalized Fourier expansion in Eq. (15). The zero-order term is not spread out by the fan-out function $\phi_f(x)$ and produces in the far field a single peak on the optical axis. Since the amplitude of one fan-out order scales as $(\eta/N)^{0.5}$ with increasing fan-out number N, the interference of the central fan-out order with the zero-order peak on the optical axis can no longer be compensated. As shown in Ref. 3, further improvement is possible by shifting the fan-out array off axis and separating the fan-out orders from the zeroth order. A lateral shift of half the spot spacing $\Delta x'$ in the far field, which corresponds to the addition of a linear phase varying from 0 to π over one period of the fan-out function $\phi_f(x)$, is sufficient to reduce the uniformity-error sensitivity σ_s of the 45×1 fan-out element to about 15%, as shown in Fig. 5. In this special case, the dependence of the uniformity sensitivity σ_s on the phase offset φ_0 has a periodicity of π, since only odd-numbered (q) terms of the generalized Fourier expansion overlap with the fan-out diffraction orders in the far field.

Scaling errors have only a small influence on the diffraction efficiency of fan-out elements in the far field. This holds for continuous and wrapped fan-out phase functions. Note that due to the presence of uniformity errors, the efficiency can even increase above the efficiency of the ideal fan-out function η.

3.2 *Focusing Fan-out Elements*

Adding focusing power $\phi_s(x)$ to the fan-out function increases the number of 0-2π transitions in the phase function. Therefore, a further improvement in the sensitivity of the uniformity error to scaling errors can be expected. This behavior has been demonstrated experimentally in a previous publication.[12] For the analysis of focusing fan-out elements, we have calculated the Fresnel propagation of the scaled transmittance function into the detection plane. By inserting Eqs. (5) and (15) into Eq. (6), we obtain for the Fresnel propagation of the scaled transmittance function $t_s(x;\lambda)$

$$U(x',z) = \frac{1}{\sqrt{i\lambda z}} \sum_{q=-\infty}^{\infty} \exp[iq(\varphi_0 - \pi)]\ \mathrm{sinc}(\alpha - q)$$

$$\times \int_{-\infty}^{\infty} P(x)\ \exp[iq\phi_f(x)]\ \exp\left[i\pi x^2\left(\frac{1}{\lambda z} - \frac{q}{\lambda_0 f}\right)\right]$$

$$\times \exp\left(-i\frac{2\pi}{\lambda z}xx'\right)\,dx\,, \tag{18}$$

where multiplicative phase factors have been omitted. Similarly to the analysis of the blazed Fresnel zone plate,[9,11] the diffraction orders q of the generalized Fourier series expansion are focused in different planes at the locations

$$z_q = \frac{\lambda_0 f}{\lambda q}\,. \tag{19}$$

The fan-out pattern is focused in the plane $z_1 = \lambda_0 f/\lambda$. The spot spacing $\Delta x'(z = z_1)$ of the fan-out orders in the plane $z = z_1$ can be calculated from Eqs. (18) and (19):

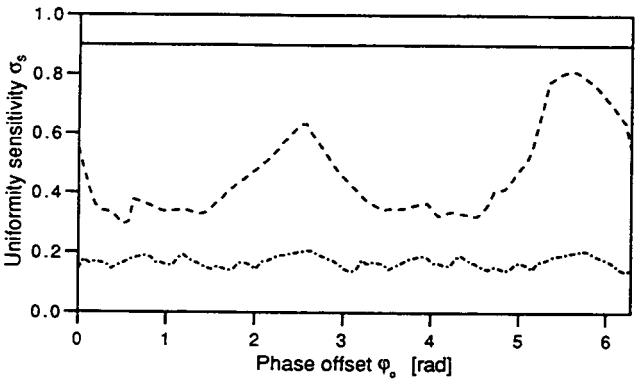

Fig. 5 Uniformity-error sensitivity σ_s for the 45×1 fan-out element as a function of the phase offset parameter φ_0. Dashed curve: phase function with 0–2π transitions; dash-dot curve: off-axis reconstruction of the fan-out function by half the spot spacing distance $\Delta x'$. The value of σ_s for the continuous phase function is indicated for comparison (solid curve).

$$\Delta x'(z=z_1)=\frac{\lambda z_1}{d}=\frac{\lambda_0 f}{d} \quad . \tag{20}$$

Therefore, in contrast to Fourier-transform elements, focusing fan-out elements have the property that the spot spacing in the focal plane z_1 is independent of the readout wavelength λ. However, focusing fan-out elements are not achromatic, because the focal-plane position z_1 depends on the readout wavelength λ.

The defocusing of spurious noise diffraction orders in the focal plane z_1 of the fan-out function produces a continuous noise distribution and increases the signal-to-noise ratio. We have calculated the uniformity error sensitivity σ_s and the efficiency η_s of the focusing 9×1 fan-out element as a function of the focal length $z_1=f$ for the parameters $\lambda=\lambda_0=0.6328$ μm, $D=2.56$ mm, and $d=160$ μm. The results have been obtained for a fixed value of the phase offset φ_0 and are represented in Figs. 6(a) and 6(b). On the top axis in Fig. 6(a) and 6(b), we have given the reciprocal of the Fresnel number $N_f=D^2/(4\lambda f)$ for the focusing term $\phi_s(x)$ in the phase function $\Psi(x)$. The transition between the far-field and the near-field behavior can clearly be seen in both curves. The fluctuations for $f<10^3$ mm and $N_f>2.6$ indicate that the zero-order term is sufficiently defocused over more than one fan-out order. Thus, the fan-out performance is determined by the interference with a continuously distributed background noise. The efficiency η_s converges for decreasing f to the value $\eta_s=(\mathrm{sinc}^2 0.1)\eta=0.961$ predicted by Eq. (15). In this limit, the interference effects on the efficiency and the uniformity become negligible.

Similarly to the case of Fourier-transform fan-out elements, the uniformity-error sensitivity of focusing elements can be minimized by optimizing the phase offset φ_0. It is important to note that even a weak focusing power adds sufficient supplementary transition points to the phase function to create fan-out elements that are almost independent of scaling errors. This result is shown in Fig. 7, where the uniformity-error sensitivity σ_s is plotted as a function of the phase offset φ_0 for a focusing 9×1 fan-out element with a focal length of $f=10^3$ mm, which corresponds to a small Fresnel number of $N_f=2.6$. For an optimum choice of φ_0, a uniformity-error sensitivity σ_s below 2% can be achieved.

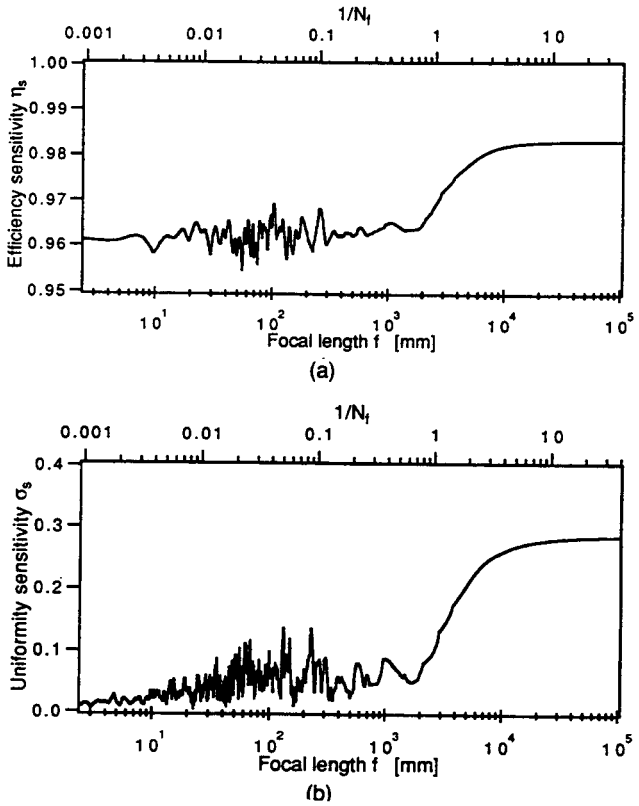

Fig. 6 (a) Efficiency sensitivity η_s and (b) uniformity error sensitivity σ_s for the focusing 9×1 fan-out element as a function of the focal length f and the reciprocal of the Fresnel number N_f. The curves are calculated for a fixed value of the phase offset parameter φ_0.

As shown in this section, the optimization of the position of the 0-2π transition points in the kinoform relief reduces efficiently the sensitivity of the uniformity error to profile scaling errors. The position of the transition points can be optimized through the phase offset φ_0, which is therefore an important parameter for the fabrication of high-quality fan-out elements by direct-write technologies.

4 Fabrication by Laser-Beam Writing

Our approach for the fabrication of kinoform DOEs is direct laser-beam writing in photoresist. By using successive replication of the master photoresist microrelief, this technology has the potential for low-cost mass fabrication. The laser-beam writing system at the Paul Scherrer Institute is described in detail in Refs. 1, 13, and 14. It uses for the writing an x-y raster scan movement that allows the realization of arbitrary two-dimensional structures. The resist is exposed by a focused HeCd laser beam at the wavelength $\lambda=442$ nm. The writing-spot diameter has been determined to $\delta=1.6$ μm at $1/e$ intensity points by knife-edge measurements. For relief depths $h\leq 3$ μm the Shipley Microposit S1828 photoresist is used, which after exposure is developed for 30 s, using the Shipley AZ 303 developer diluted 1:10 with de-ionized water. This process results in a very linear characteristic of relief depth versus exposure energy. Therefore, small errors during the exposure and the development process produce the linear relief scaling errors, which we consider for the fabrication-error analysis.

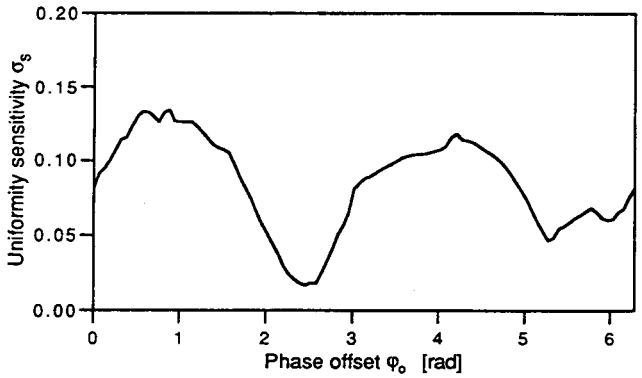

Fig. 7 Uniformity error sensitivity σ_s as a function of the phase offset parameter φ_0 for the focusing 9×1 fan-out element with diameter $D=2.56$ mm, fan-out period $d=160$ μm, wavelength $\lambda=0.6328$ μm, and focal length $f=1000$ mm.

The finite spot size of the laser-beam writer does not allow sharp steps at the 0–2π transitions in the surface-relief profile. The resulting surface relief can be described by a convolution of the ideal shape and the focused writing spot of diameter δ. The smoothed transitions have a width approximately equal to δ. For small diameters δ on the order of the wavelength, the smoothed transitions in the surface relief can no longer be accurately described by amplitude transmittance and paraxial scalar diffraction theory. However, if we assume that the minimum segment size s between two transitions is much larger than δ, paraxial scalar diffraction theory gives accurate results. In this limit, we describe the resulting phase function $\Psi_c(x)$ after the surface-relief element directly by a convolution of the ideal phase function $\Psi(x)$ and a Gaussian point spread function (PSF), namely,

$$\Psi_c(x)=\Psi(x)*g(x)\ , \tag{21}$$

where $*$ represents the convolution operation and

$$g(x)=\sqrt{\pi}\frac{\delta}{2}\exp\left(-\frac{4x^2}{\delta^2}\right) \tag{22}$$

is the normalized PSF of the laser-beam writing system. The consequences for the profile shape are shown in Fig. 8, where the ideal phase function $\Psi(x)$ and the resulting phase function $\Psi_c(x)$ after the convolution are shown. The laser-beam writing process introduces rounded transitions and reduces the modulation depth. As a consequence, the diffraction efficiency and the uniformity of the ideal phase function are reduced. We have analyzed how these PSF effects can be compensated. In addition, we have verified whether they change the optimized scaling error behavior of the kinoform function, which was derived in Sec. 3 for perfect transitions.

For this purpose, we have calculated the Fresnel propagation [Eq. (6)] of the convolved phase function $\Psi_c(x)$ for the focusing 9×1 fan-out element into the focal plane z_1. The calculated diffraction efficiency η and the uniformity error σ are shown in Fig. 9(a) and 9(b) as a function of the focal length $z_1=f$ and the reciprocal of the Fresnel number N_f of the focusing element. The results have been calculated for $\lambda=\lambda_0=0.6328$ μm, $D=2.56$ mm, $d=160$ μm, $\delta=1.6$ μm, and for a fixed phase offset value φ_0. We observe a

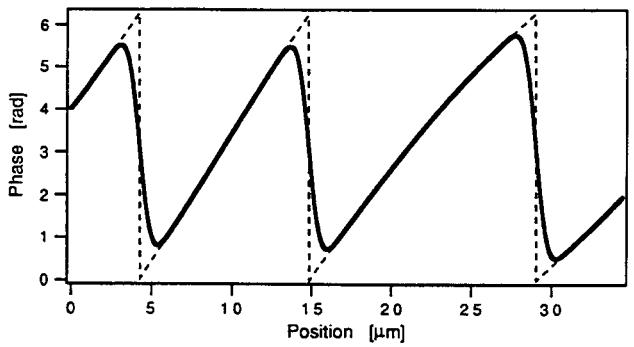

Fig. 8 Influence of the writing-spot diameter δ on profile shape. Dashed curve: ideal phase function $\Psi(x)$; solid curve: resulting phase function $\Psi_c(x)$ after convolution with the Gaussian PSF of diameter $\delta=1.6$ μm at $1/e$ intensity points.

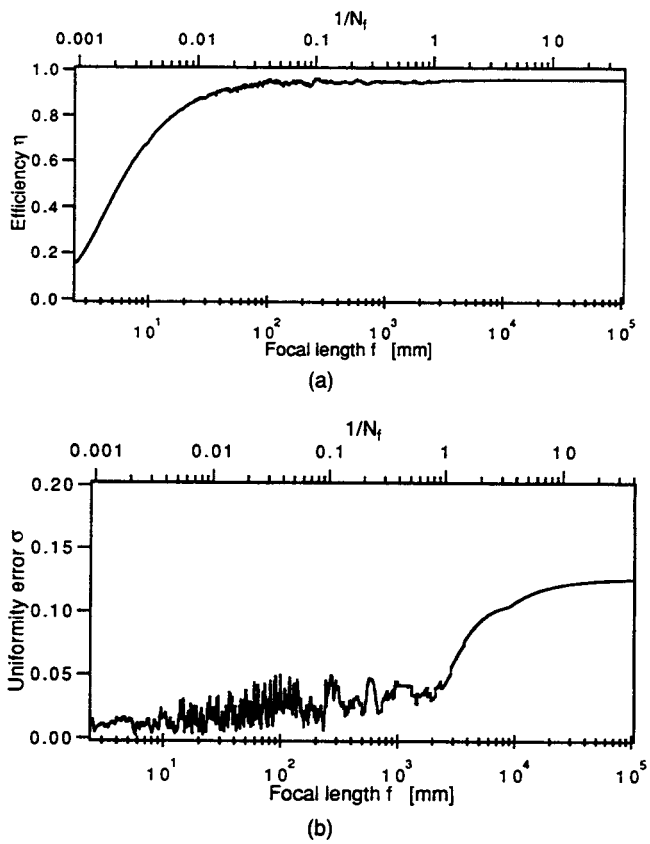

Fig. 9 (a) Efficiency η and (b) uniformity error σ as a function of the focal length f and the reciprocal of the Fresnel number N_f, produced by the phase function $\Psi_c(x)$ of the focusing 9×1 fan-out element after convolution with the Gaussian PSF. The curves are calculated for a fixed value of the phase offset parameter φ_0.

reduction of the diffraction efficiency η that is proportional to the number of transition points in the surface-relief profile. This efficiency loss becomes the major problem for the realization of focusing elements with F numbers $f/D\leq10$. In this case, PSF compensation[15] and clipping of the phase function $\Psi(x)$ to a multiple of 2π have to be considered. The uniformity error decreases with increasing focal length f. Even for weak focusing power, focusing kinoform elements behave similarly to off-axis elements,[3] where the signal phase

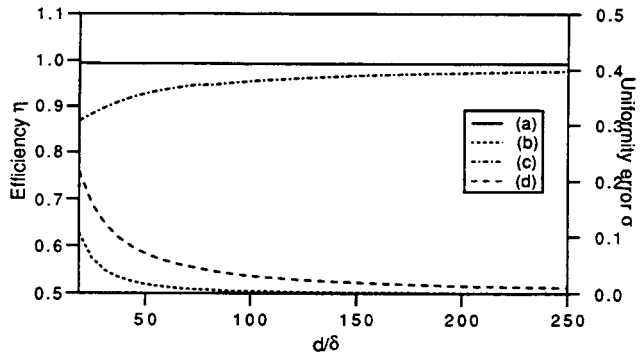

Fig. 10 Efficiency η and uniformity error σ of the convolved phase $\Psi_c(x)$ as a function of the ratio of the fan-out period d to the writing-spot diameter δ for the 9×1 fan-out element: (a) efficiency and (b) uniformity error of the continuous phase function; (c) efficiency and (d) uniformity error of the phase function with optimized 0–2π transitions.

is encoded by the position of the transition points (detour-phase principle). As a consequence, the rounding of the transitions has only a small influence on the uniformity provided that the center of the transition remains at the correct position. Therefore, the optimized set of transition points, obtained for the ideal phase function $\Psi(x)$, also yields the best scaling-error tolerances and should be used for the fabrication of focusing fan-out elements.

For the analysis of Fourier-transform fan-out elements, we have calculated the Fraunhofer diffraction pattern of the convolved phase function $\Psi_c(x)$. The influence of the convolution with the writing-spot size has been analyzed for continuous-phase fan-out elements and fan-out elements with optimized 0–2π transitions. Figure 10 plots the efficiency η and the uniformity error u for the 9×1 fan-out element, after convolution for both types, versus the ratio of the grating period d to the writing-spot diameter δ.

For continuous-phase elements, the efficiency η (solid line) is almost independent of the ratio d/δ. However, the uniformity error σ (dashed line) increases for small d/δ. For $d/\delta > 200$, the remaining small uniformity error σ is essentially due to a small scaling error, which can be directly compensated to achieve perfect uniformity again. This is no longer possible for smaller d/δ, because the convolution changes the profile shape. In this case, the convolution operation has to be directly included in the design algorithm for the fan-out phase function $\phi_f(x)$. For this purpose, we use an iterative approach, as described in Ref. 16, and can achieve perfect uniformity and high diffraction efficiency in the case of the 9×1 fan-out element for $d/\delta \geq 10$. For $d/\delta < 10$, uniform fan-out solutions can be found, but no longer with the optimized shape of Fig. 1 and therefore with lower diffraction efficiency.

For fan-out solutions with optimized transitions, the efficiency loss for low $d/\delta < 30$ becomes the main problem. In addition, the optimized scaling-error behavior starts to fail at about the same limit. For $d/\delta < 100$, the position of the transition points for optimized scaling-error behavior starts to depend on the width δ of the PSF. Therefore, in this domain, the position of the transition points has to be reoptimized by taking into account the convolution with the writing-spot size. For still smaller $d/\delta < 30$, the solution behaves like a continuous-phase function. In this case, the scaling-error tolerances can no longer be optimized, and only poor diffraction efficiencies are achieved.

In conclusion, it is reasonable to fabricate Fourier-transform fan-out elements with small ratios d/δ as continuous-phase gratings, in order to achieve high diffraction efficiency. For larger d/δ, it is preferable to introduce discrete transitions into the phase function and optimize the scaling-error behavior, as shown in Sec. 3, in order to achieve better fabrication-error tolerances. The above limits have been calculated for the 9×1 fan-out element. However, numerical simulations have shown that the critical values of d/δ are proportional to the fan-out number N.

5 Experimental Results

Experimental results have been achieved for the fabrication of cylindrically focusing 9×1 fan-out elements in photoresist. The elements have been designed for the wavelength $\lambda_0 = 0.6328$ μm, with a diameter $D = 2.64$ mm, a fan-out period $d = 165$ μm, and focal length $f = 25$ mm, which corresponds to an F number ≈ 10. This results in a smallest segment size of $s = 12$ μm at the border of the structure. In order to use a standard fabrication process for the laser-beam writer, the phase function has been rounded to a 1×1-μm^2 pixel grid. Smaller pixel sizes are possible, but increase the writing time of the structure. The rounding shifts the position of the transition points and introduces detour-phase errors to the signal phase function. However, since the local phase error is not repetitive for focusing elements, the rounding operation produces a negligible uniformity error ($< 1\%$). Figure 11 shows an atomic-force microscope measurement of the profile shape in the central region of the focusing fan-out element. Clearly visible is the surface roughness, which is due to the varying overlap between neighboring scan lines due to positioning errors along the scan movement. We have fabricated on the same substrate eight different fan-out elements with varying exposure energy, linearly scaled with factors α from 0.85 to

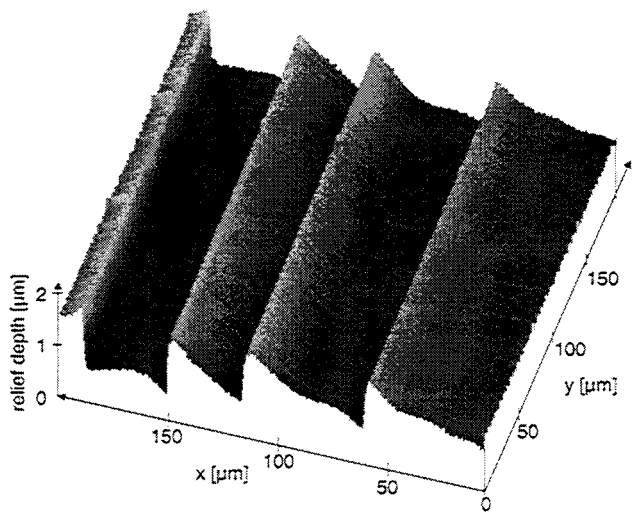

Fig. 11 AFM measurement of the profile in the central region of a cylindrical focusing 9×1 fan-out element designed for the wavelength $\lambda = 0.6328$ μm with diameter $D = 2.64$ mm, fan-out period $d = 165$ μm, and focal length $f = 25$ mm.

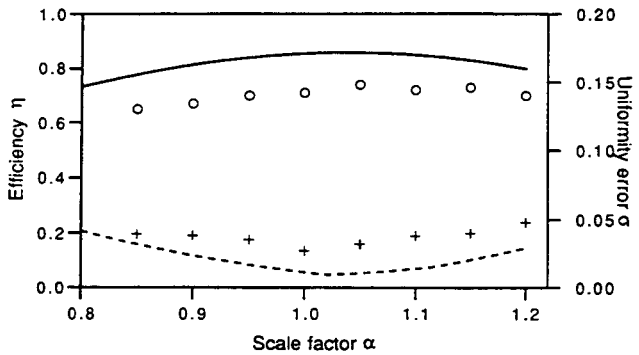

Fig. 12 Efficiency η and uniformity error σ of the fabricated element as a function of the scaling factor α. Solid curve: calculated efficiency; dashed curve: calculated uniformity error; ○: measured efficiency; +: measured uniformity error.

1.20. In Fig. 12, we have represented the measured efficiency η and the measured uniformity error σ of the eight elements, as well as the simulated scaling behavior of the ideal phase function convolved with the Gaussian PSF of diameter $\delta = 1.6$ μm. Good agreement between the experimental results and the theoretical data is observed. Note that for a nonoptimized choice of the transition points, the scaling-error behavior can be 10 times worse. The measured uniformity error is smaller than 5%, even for a large scaling error of 20%. A maximum diffraction efficiency of 74% has been measured (compensated for the Fresnel reflection at the photoresist-air and glass-air interfaces). The 10% efficiency loss compared to the calculated values is due to the scattered light from the surface roughness. As shown in Fig. 12, the surface roughness has a basic periodicity equal to the interscan distance (1 μm). Therefore, the major quantity of scattered light is diffracted out of the fan-out signal pattern and does not affect the uniformity.

6 Conclusions

Continuous-phase DOEs can be calculated by using design concepts based on either geometrical optics or physical optics. The resulting continuous phase function can always be wrapped to an integer multiple m of 2π, in order to reduce the modulation depth and to enable the realization by a planar surface-relief DOE. In the ideal case, the phase wrapping has no influence on the optical performance of the element. However, the phase wrapping and, in particular, the position of the transition points determine the stability of the kinoform phase function against fabrication errors. In this paper, we have shown that in the case of kinoform DOEs that produce a discrete intensity distribution in a desired image plane, the position of the 0–$2\pi m$ transition points in the phase function can be optimized in order to achieve high tolerance of the kinoform reconstruction quality against vertical profile scaling errors. As a result of this optimization process, the sensitivity of fan-out kinoforms to profile scaling errors can be reduced by about a factor 10. Scaling errors represent a major problem in the fabrication of kinoform surface reliefs by direct-write techniques. As a consequence, fabrication-error tolerances and scaling-error optimization should be included in the design of the phase function, in order to realize high-quality elements.

Numerical results have been presented for the design of Fourier-transform and focusing fan-out elements that enable high diffraction efficiency and have optimized profile scaling-error tolerances. The fabrication of such elements by laser-beam writing is discussed, and limits for the validity of the fabrication-error tolerance optimization are derived. Experimental results have been achieved for the fabrication of focusing 9×1 fan-out elements by laser-beam writing in photoresist. Uniformity errors smaller than 5% for profile scaling errors up to 20% have been demonstrated.

References

1. M. T. Gale, M. Rossi, H. Schütz, P. Ehbets, H. P. Herzig, and D. Prongué, "Continuous-relief diffractive optical elements for two-dimensional array generation," *Appl. Opt.* **32,** 2526–2533 (1993).
2. J. M. Miller, M. R. Taghizadeh, J. Turunen, N. Ross, E. Noponen, and A. Vasara, "Kinoform array illuminators in fused silica," *J. Mod. Opt.* **40,** 723–732 (1993).
3. J. Turunen, J. Fagerholm, A. Vasara, and M. R. Tagizadeh, "Detour-phase kinoform interconnects: the concept and fabrication considerations," *J. Opt. Soc. Am. A* **7,** 1202–1208 (1990).
4. M. Larsson, M. Ekberg, F. Nikolajeff, and S. Hard, "Successive-development optimization of resist kinoforms manufactured with direct-writing electron-beam lithography," *Appl. Opt.* **33,** 1176–1179 (1994).
5. Y. Oppliger, P. Sixt, J. M. Stauffer, J. M. Mayor, P. Regnault, and G. Voirin, "One-step shaping using gray-tone mask for optical and microelectronic applications," *Microelectron. Eng.* **23,** 449–454 (1994).
6. U. Krackhardt, J. N. Mait, and N. Streibl, "Upper bound on the diffraction efficiency of phase-only fan-out elements," *Appl. Opt.* **31,** 27–37 (1992).
7. H. Lüpken, T. Peter, F. Wyrowski, and O. Bryngdahl, "Phase synthesis for array illuminator," *Opt. Commun.* **91,** 163–167 (1992).
8. J. W. Goodman, *Introduction to Fourier Optics,* McGraw-Hill, New York (1968).
9. D. A. Buralli, G. M. Morris, and J. R. Rogers, "Optical performance of holographic kinoforms," *Appl. Opt.* **28,** 976–983 (1989).
10. J. W. Goodman and A. M. Silvestri, "Some effects of Fourier-domain phase quantization," *IBM J. Res. Dev.* **14,** 478–484 (1970).
11. H. Dammann, "Blazed synthetic phase-only holograms," *Optik* **31,** 95–104 (1970).
12. M. Rossi and R. Kunz, "Focusing fan-out elements based on phase-matched Fresnel lenses," *Opt. Commun.* **112,** 258–264 (1994).
13. M. T. Gale, G. K. Lang, J. M. Raynor, H. Schütz, and D. Prongué, "Fabrication of kinoform structures for optical computing," *Appl. Opt.* **31,** 5712–5715 (1992).
14. M. T. Gale, M. Rossi, J. Pedersen, and H. Schütz, "Fabrication of continuous-relief micro-optical elements by laser beam writing in photoresist," *Opt. Eng.* **33,** 3556–3566 (1994).
15. M. Ekberg, F. Nikolajeff, M. Larsson, and S. Hard, "Proximity-compensated blazed transmission grating manufacture by direct-writing electron beam lithography," *Appl. Opt.* **33,** 103–107 (1994).
16. J. Bengtsson, "Direct inclusion of the proximity effect in the calculation of kinoforms," *Appl. Opt.* **33,** 4993–4996 (1994).

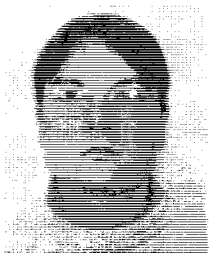

Peter Ehbets received the diploma in physical electronics from the University of Neuchâtel, Switzerland, in 1990. Then he joined the Applied Optics Group at the Institute of Microtechnology of the University of Neuchâtel as a graduate research assistant. In 1995, he received the PhD degree in optics from the University of Neuchâtel. His current research deals with the design and fabrication of diffractive optical elements for beam shaping and optical interconnects.

Markus Rossi received his MSc degree in physics at the Swiss Federal Institute of Technology (ETH), Zürich, Switzerland, in 1990. He is currently working at the Paul Scherrer Institute in Zürich on the design, fabrication, and characterization of micro-optical elements. In 1995, he received the PhD degree in optics from the University of Neuchâtel, Switzerland. His work includes the study of novel types of planar optical elements in the form of phase-matched Fresnel elements and their fabrication by laser-beam writing. Special interest is devoted to applications of micro-optical elements for optical interconnection systems.

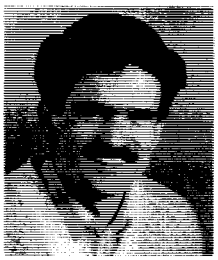

Hans Peter Herzig received the diploma in physics from the Swiss Federal Institute of Technology in Zürich (ETHZ), Switzerland, in 1978. From 1978 to 1982 he was a scientist in the Optics Development Department of the company Kern in Aarau, Switzerland, where he worked in lens design and optical testing. In 1983, he joined the Applied Optics Group at the Institute of Microtechnology of the University of Neuchâtel, Switzerland, as a graduate research assistant, working in the field of holographic optical elements, especially scanning elements. In 1987, he received the PhD degree in optics from the University of Neuchâtel. Now he is lecturing on modern optics and is responsible for research in micro-optics, including diffractive optical elements and microlenses.